Histochem Cell Biol (2009) 132:199–210
DOI 10.1007/s00418-009-0588-y

ORIGINAL PAPER

Doxycycline accelerates renal cyst growth and fibrosis in the *pcy/pcy* mouse model of type 3 nephronophthisis, a form of recessive polycystic kidney disease

Larissa Osten · Marion Kubitza · Anna Rachel Gallagher · Jürgen Kastner · Heike Olbrich · Uwe de Vries · Frieder Kees · Brigitte Lelongt · Stefan Somlo · Heymut Omran · Ralph Witzgall

Accepted: 18 March 2009 / Published online: 21 April 2009

Abstract Nephronophthisis belongs to a family of recessive cystic kidney diseases and may arise from mutations in multiple genes. In this report we have used a spontaneous mouse mutant of type 3 nephronophthisis to examine whether the doxycycline-inducible synthesis of Timp-2, a natural inhibitor of matrix metalloproteinases, can influence renal cyst growth in transgenic mice. Metalloproteinases may exert either a negative or a positive effect on the progression of cystic kidney disease, and we reasoned that this may be most effectively examined by using a natural inhibitor. Surprisingly, already the application of doxycycline, which also inhibits matrix metalloproteinases, accelerated renal cyst growth and led to increased renal fibrosis, an additional effect of Timp-2 was not detected. The positive effect of doxycycline on kidney size was not due to a non-specific "anabolic effect" but was specific for cystic kidneys because it was not observed in non-cystic kidneys. When looking for potential metabolic changes we noticed that the urine of control animals led to an increase in the calcium response of LLC-PK_1 cells, whereas the urine of doxycycline-treated mice showed the opposite effect and even antagonized the urine of control animals. Further experiments demonstrated that the urine of control animals contained a heat-labile, proteinase K-resistant substance which appears to be responsible for the induction of a calcium response in LLC-PK_1 cells. We conclude that doxycycline accelerates cyst growth possibly by the induction of a substance which lowers the intracellular calcium concentration. Our data also add a note of caution when interpreting phenotypes of animal models based upon the tet system.

Keywords Doxycycline · Polycystic kidney disease · Nephronophthisis · Intracellular calcium · Primary cilia

Larissa Osten and Marion Kubitza have contributed equally.

L. Osten · M. Kubitza · J. Kastner · U. de Vries · R. Witzgall (✉)
Institute for Molecular and Cellular Anatomy,
University of Regensburg, Universitätsstrasse 31,
93053 Regensburg, Germany
e-mail: ralph.witzgall@vkl.uni-regensburg.de

A. R. Gallagher · S. Somlo
Department of Internal Medicine,
Yale University School of Medicine, New Haven, CT, USA

H. Olbrich · H. Omran
Department of Pediatrics,
University of Freiburg, Freiburg, Germany

F. Kees
Department of Pharmacology and Toxicology,
University of Regensburg, Regensburg, Germany

B. Lelongt
Inserm U702, Hôpital Tenon,
Université Pierre Et Marie Curie (Paris 6), Paris, France

Introduction

Although many genes mutated in various forms of cystic kidney diseases have been identified, it is still not clear how cysts are formed. Evidence has been presented that primary cilia, extensions of the apical plasma membrane, transmit mechanical stimuli to tubular epithelial cells and that failure to do so initiates a cystogenic program (Nauli et al. 2003; Praetorius and Spring 2001). What such a cystogenic program looks like has been an intense subject of speculation. Since the tubules and cysts are surrounded by a basement membrane and additional extracellular matrix which forms a mechanical barrier to expansion, it is reasonable to assume that the extracellular matrix has to be remodeled for

cyst formation to proceed. Matrix metalloproteinases (MMPs) and tissue inhibitors of metalloproteinases (TIMPs) represent key enzymes in the turnover of the extracellular matrix and therefore are natural candidates to modulate cyst growth. MMPs are characterized by a cysteine switch motif in the propeptide domain that keeps them in their inactive form, and by a zinc-binding motif in the catalytic domain. The two dozen different MMPs known are able to cleave a wide variety of substrates including not only extracellular matrix components but also adhesion molecules and growth factors. MMP activity is counteracted by endogenous inhibitors, the TIMPs, which inhibit virtually all MMPs by binding to them through their NH_2-terminal domain (for review see Visse and Nagase (2003)). Remarkably, one of the four TIMPs known, TIMP-2, also assists in the activation of MMP-2. The zymogen forms of MMPs are transformed into active enzymes by proteolytic cleavage. In the case of MMP-2, this occurs via formation of a trimeric complex consisting of MMP-2, TIMP-2, and a membrane-bound MMP, MT1-MMP. The MMP-2 in this trimeric complex is subsequently cleaved by free MT1-MMP (Sato et al. 1994; Strongin et al. 1995; Wang et al. 2000).

Ample data have been presented that MMPs and TIMPs are of importance in kidney diseases (Catania et al. 2007; Ronco and Chatziantoniou 2008). Circumstantial evidence that these proteins are also involved in polycystic kidney disease was presented early on when stromelysin (probably stromelysin 1 which is also known as MMP-3) was detected in cyst fluid (Gardner et al. 1991). Subsequently MMP-2, stromelysin, MMP-7, and MMP-9 were detected on tissue sections of human polycystic kidneys by immunohistochemistry (Bello-Reuss et al. 2001; Norman et al. 1995; Surendran et al. 2004). The situation becomes more complicated from the results obtained in various animal models of polycystic kidney disease. In polycystic kidneys of Han:SPRD rats, a model for autosomal-dominant polycystic kidney disease, decreased levels of Mmp-2 and increased levels of Mmp-7, Mt1-Mmp, Timp-1, and Timp-2 were detected (Obermüller et al. 2001; Riera et al. 2006; Schaefer et al. 1996). Furthermore an upregulation of Mmps and Timps was found in two models of autosomal-recessive polycystic kidney disease, specifically of Mmp-7 in the *jck*/*jck* mouse (Surendran et al. 2004), and of Mmp-2, Mmp-3, Mmp-9, Timp-1, and Timp-2 in the *cpk*/*cpk* mouse (Rankin et al. 1996, 1999). Therefore, although the expression pattern of the various MMPs obviously is complex, the MMP activity in general is higher in polycystic kidneys than in non-cystic kidneys.

Direct evidence, however, for the importance of MMPs in polycystic kidney disease is sparse. We have used batimastat, a synthetic inhibitor of various MMPs, for a therapeutic study in the Han:SPRD rat. Intraperitoneal injections of batimastat from postnatal day 14 through postnatal day 70 led to a decreased kidney weight and lower cyst number compared to vehicle-treated animals (Obermüller et al. 2001). A second study used a synthetic inhibitor of TACE, the metalloproteinase releasing soluble transforming growth factor α (TGF-α) from its membrane-bound form (Dell et al. 2001). TGF-α and other members of the epidermal growth factor (EGF) family probably contribute to cyst growth in some models of polycystic kidney disease because blockade of the EGF receptors slows down cyst formation (Sweeney et al. 2000; Torres et al. 2003). The TACE inhibitor WTACE2 indeed inhibited cystogenesis in the *bpk*/*bpk* mouse (Dell et al. 2001). These results encouraged us to extend our investigations by engineering transgenic mice which inducibly synthesize Timp-2 in the kidney. We were hoping that Timp-2 as a natural inhibitor of Mmps would show an even stronger inhibitory effect on cyst growth than batimastat.

Materials and methods

Plasmid constructs

Employing the QuikChange mutagenesis kit (Stratagene), a *Mlu* I site was introduced immediately before the stop codon of the murine Timp-2 cDNA (kind gift from Dylan Edwards) (Leco et al. 1992). This *Mlu* I site was then used to fuse a fragment coding for a HA-epitope and a stretch of nine histidines to the 3′-end of the Timp-2 cDNA. The sequence of the resulting construct Timp-2, HAHis reads as follows (the last three codons of Timp-2 are underlined, the sequence encoding the HA-epitope and the nine histidines is italicized): 5′-GAG GAC CCA ACG CGT *TAC CCA TAC GAT GTT CCA GAT TAC GCT* CGT ACT *CAC CAC CAC CAC CAC CAC CAC CAC CAC* CGT ACG TAA-3′.

Finally, the Timp-2, HAHis fragment was transferred into the expression plasmids pUHD 10-3 and pBI-3 (kind gift from H. Bujard) (Baron et al. 1995) which permit the doxycycline-inducible synthesis of the HA-epitope- and histidine-tagged Timp-2 protein. Whereas pUHD 10-3 only controls the synthesis of the tagged Timp-2 protein, pBI-3 contains a bi-directional expression cassette consisting of the *nLacZ* gene (encoding β-galactosidase with a nuclear localization signal) and the mutated Timp-2 cDNA.

Stable transfections and protein purification

HtTA-1 cells, which are HeLa cells producing the tetracycline-dependent transactivator, were stably transfected with the pUHD 10-3/Timp-2, HAHis construct using a poly-ornithine protocol (Dong et al. 1993). Forty-eight

hours after transfection, cells were plated onto 10-cm petri dishes and selected with puromycin (0.5 μg/ml; Calbiochem, Darmstadt, Germany). Approximately 2 weeks later resistant colonies were isolated and tested for the synthesis of the tagged Timp-2 protein. Individual clones were expanded and induced by removal of doxycycline. The medium was collected, purified over a nickel column and then subjected to Western blot analysis with the mouse monoclonal anti-HA-epitope antibody 12CA5 (cell culture supernatant diluted 1:30).

Reverse zymography

Purified epitope-tagged Timp-2 was electrophoresed under non-reducing conditions on 8% SDS-polyacrylamide gel co-polymerized with 1 mg/ml of gelatin. When the run was complete, the gel was washed twice for 30 min each in 2.5% Triton X-100 to remove SDS and then incubated in substrate buffer (50 mM Tris–HCl pH 7.5, 5 mM $CaCl_2$, and 1 μM $ZnCl_2$) enriched with concentrated media from a rabbit collecting duct cell line producing Mmp-2 and Mmp-9 (Piedagnel et al. 1999). Finally the gel was stained for 30 min at room temperature in 0.5% Coomassie brilliant blue G, 40% methanol, 10% acetic acid, and destained in 40% methanol, 1% acetic acid.

Timp-2 transgenic mice

The linearized pBI-3/mTimp-2, HAHis plasmid was injected into fertilized oocytes of C57Bl/6 × DBA mice. Founders were identified by screening tail biopsies for the presence of *nLacZ* by Southern blot according to standard protocols (Ausubel et al. 1996). Ten micrograms of genomic DNA was digested with *Bam*H I and hybridized with the *nLacZ* fragment. Individual lines were first maintained on a C57BL/6 background to expand the colony. Later on they were first mated with $rtTA^{LAP}$-1 mice to obtain mice containing the expression cassettes for both the tagged Timp-2 protein and the reverse tetracycline-dependent transactivator. Transgenic mice with both expression cassettes were subsequently crossed twice with $CD1^{pcy/pcy}$ mice to maintain the two expression cassettes on a $CD1^{pcy/pcy}$ background. In order to differentiate between the wild-type and mutant *Nphp3* alleles, genomic DNA was isolated from mouse tails and amplified with oligonucleotides ex12 (F) 5′-CCACAGTGAGGATGGAAAGG-3′ and ex12 (R) 5′-TGCTAATAGAAGACACAGTGAGAGC-3′. The PCR product was analyzed by bi-directional sequencing.

The transgene was induced by administering doxycycline hydrochloride (Sigma, Deisenhofen, Germany) at a concentration of 2 mg/ml together with 5% sucrose in the drinking water (Gallagher et al. 2003). The doxycycline/sucrose solution was prepared fresh every Monday and Friday in a brown drinking bottle. At the end of the treatment period, mice were perfused through the distal abdominal aorta with 4% paraformaldehyde, 1× PBS for 3 min at a pressure of 180 mm Hg. The kidneys and the heart were removed and weighed. Individual pieces of each kidney were either immersed for several hours in 18% sucrose, 1× PBS, and frozen away at −80°C, or they were fixed overnight in 4% paraformaldehyde, 1× PBS, and embedded in paraffin.

Pkhd1 knock-out mice

The *Pkhd1* knock-out mice have been described recently. They contain a deletion in exon 4 of the gene and develop polycystic liver but not polycystic kidney disease (Gallagher et al. 2008). Starting at the age of 1 month and lasting for 8 weeks, $Pkhd1^{del4/del4}$ knock-out mice received 2 mg/ml of doxycycline together with 5% sucrose in the drinking water, whereas control animals of the same genotype only received 5% sucrose. The solutions were prepared fresh for every 3 days in a brown drinking bottle. At the end of the treatment period, the kidneys and livers were removed, weighed, and finally fixed overnight in 4% paraformaldehyde and 1× PBS before being embedded in paraffin.

Determination of doxycycline concentration

Kidneys were homogenized in liquid nitrogen. Then an aliquot of 100 mg of pulverized tissue was extracted with 500 μl of trichloroaceticacid/McIlvaine buffer (Cinquina et al. 2003) using demeclocycline as an internal standard. In order to deproteinize the tissue suspension, 125 μl of perchloric acid/acetonitrile were added (Kees et al. 1990) and the precipitated protein was removed by centrifugation. The doxycycline concentration in the supernatant was determined by HPLC and photometric detection at 344 nm as described previously (Kees et al. 1990). An analogous protocol was employed to measure the doxycycline concentration in the serum.

Histological analysis

Histochemical staining for β-galactosidase was carried out on 7 μm cryosections. The sections were equilibrated in staining solution (5 mM potassium ferricyanide, 5 mM potassium ferrocyanide, 2 mM $MgCl_2$, 20 mM NaCl, 10 mM EGTA pH 8.0, and 10 mM sodium phosphate pH 8.0) and then incubated overnight at room temperature in the presence of 1 mg/ml of X-gal. The sections were washed twice in PBS and then counterstained with eosin and mounted.

Staining with Sirius red was carried out on paraffin sections. After deparaffinization, sections were rinsed briefly in deionized water and then stained for 45 min in a solution obtained by mixing one volume of 1 g/ml of Sirius red (cat. no. 365548-5G, Aldrich) and five volumes of saturated picric acid. Then the sections were rinsed for 5 min in 70% ethanol and twice for 5 min in 100% ethanol, equilibrated for 2 × 5 min in xylene, and mounted.

Morphometry

To determine the relative area occupied by cysts, kidney sections were deparaffinized and then stained with hematoxylin and eosin. Whole kidney pictures were analyzed with ImageJ version 1.38 (Abramoff et al. 2004) or with MetaMorph 7.1.7 (Molecular Devices, Downingtown, PA, USA) by determining the total kidney area and the area not stained with H&E.

To determine the relative fibrotic area, sections were stained with Sirius red. Pictures were taken with a 5× objective and automatically assembled using the Mosaix software from Carl Zeiss. Whole kidney pictures were analyzed with ImageJ by determining the total kidney area and the area stained with Sirius red.

Quantitative PCR

After RNA was extracted from kidneys using the Nucleospin RNA L kit (Macherey-Nagel) it was reverse-transcribed into cDNA with the iScript cDNA synthesis kit (BioRad) following the manufacturer's recommendations. Quantitative PCR was performed on a Rotor-Gene 3000 (Corbett Research) with 10 ng of the cDNA using HotStarTaq (Qiagen) and the following oligonucleotides: Timp2-F1 (5′-GAC ATG ATA AGA TAC ATT GAT GAG TTT GG-3′) and Timp2-R1 (5′CAT TTT TTT CAC TGC ATT CTA GTT GTG-3′) for Timp-2, LacZ-F1 (5′-CCG TCT GAA TTT GAC CTG AGC-3′) and LacZ-R1 (5′-CAA CGA GAC GTC ACG GAA AA-3′) for LacZ, and S9-fwd (5′-GCAAGATGAAGCTGGATTAC-3′) and S9-rev (5′-GGGATGTTCACCACCTG-3′) for S9. In the case of Timp-2, the reverse primer was selected from the transgene-specific 3′ non-translated region to distinguish between the exogenous and endogenous Timp-2 mRNAs. Data were normalized to S9 ribosomal mRNA and expressed as relative mRNA levels.

Primary cultures of kidney epithelial cells and collagen gels

Adult CD1$^{pcy/pcy}$ mice were killed by cervical dislocation. The kidneys were removed, rinsed briefly in ice-cold PBS and immediately placed into DMEM/F12. After the kidneys were cut with a scissors into small pieces, the suspension was centrifuged for 5 min at 100*g* and the pellet was resuspended in 1 ml of DMEM/F12, 2 mg/ml of dispase II (Roche Diagnostics), 1.4 mg/ml of collagenase A (Roche Diagnostics), 0.2 mg/ml of DNase I (Roche Diagnostics), 5 mM $MgCl_2$, 1 mM $CaCl_2$, 100 U/ml of penicillin, and 100 µg/ml of streptomycin. The tissue was digested for 1 h at 37°C, separation was facilitated by pipetting the suspension up and down every 15 min. Then the suspension was centrifuged for 5 min at 100*g*, washed in DMEM/F12, and resuspended in 14 ml of DMEM/F12, 10% fetal calf serum, 1× insulin–transferrin–selenite supplement (Invitrogen), 100 U/ml of penicillin, and 100 µg/ml of streptomycin. Debris was allowed to settle by leaving the suspension in an upright position for 3 min before 12 ml of the supernatant was taken off and transferred into 25-cm^2 tissue culture flasks.

Collagen gels

Adherent primary cell cultures from passages 1–3 were trypsinized, resuspended in rat tail collagen I (BD Biosciences) and plated into 96-well plates. After 1 week cells were fixed for 60 min with 1× PBS, 2% glutaraldehyde, stained for 30 min with 1× PBS, 20 µg/ml of propidium iodide, and washed twice with 1× PBS. Finally the collagen gel was embedded in 1% agarose and nuclei were analyzed in a Zeiss LSM 510 laser scanning microscope. Cystic structures were visualized over the whole height of the collagen gel.

Calcium imaging

CD1$^{pcy/pcy}$ mice were administered doxycycline at a concentration of 2 mg/ml via the drinking water for 10 days (together with 5% sucrose; control mice received only 5% sucrose). On the last day, urine was collected over a period of 22 h (from 11:30 a.m. to 9:30 a.m.) by placing the animals in metabolic cages. For intracellular calcium measurements, the urine was diluted to a final concentration of 5% (vol/vol) in imaging buffer containing 150 mM NaCl, 5 mM KCl, 2.2 mM $CaCl_2$, 5 mM glucose, 10 mM Hepes pH 7.4, and 1 mM $MgCl_2$. When indicated, urine aliquots were incubated for 15 min at 95°C and treated with 100 µg/ml of proteinase K for 30 min at 37°C, respectively. The diluted urine was applied to LLC-PK_1 cells grown on cover slips. Before starting the measurements, the cells were washed twice in imaging buffer and then loaded for 30 min at room temperature in imaging buffer to which 5 mM probenecid, 0.025% pluronic (Invitrogen), and 5 µM Fura-2 AM (Invitrogen) were added. Fluorescence was measured by alternating between the excitation wavelengths of 340 nm and 380 nm and measuring the emitted light every second for 10 min.

Mass spectrometry

Proteins were separated on denaturing polyacrylamide gels and stained with Coomassie Brilliant Blue. Subsequently the bands of interest were excised, completely destained, and digested in the gel using trypsin (sequencing grade; Roche Diagnostics GmbH, Mannheim, Germany). The digests were analyzed by peptide mass fingerprints and MS/MS spectra of selected peptides (combined MS + MS/MS search) using a 4800 Proteomics Analyzer (ABI). Proteins were identified searching the non-redundant National Center for Biotechnology Information (NCBI) database (downloaded September 2008) using the Mascot search program (Matrix Science Ltd, London, England). Protein scores higher than 80 were considered statistically significant ($P < 0.05$; score: $-10 \times \log(P)$; P is the probability that the observed match is a random event).

Statistical analysis

All values are presented as mean ± standard deviation. Statistical analysis was done through the *t*-test procedure. Differences were considered significant when $P \leq 0.05$.

Results

Generation of a HA- and histidine-tagged Timp-2 protein

Although we were able to demonstrate that the treatment of Han:SPRD rats with the metalloproteinase inhibitor batimastat slowed down renal cyst progression, the effect was moderate (Obermüller et al. 2001). Possibly a more potent metalloproteinase inhibitor would have resulted in a more pronounced beneficial effect which is why we wanted to test an endogenous inhibitor such as Timp-2 in transgenic animals. In order to be able to discern between the endogenous and the transgene-encoded Timp-2 proteins, we generated a recombinant Timp-2 protein containing a HA-epitope and nine histidines at its COOH-terminus. Since TIMPs bind to MMPs through their NH_2-terminal domain (Murphy et al. 1991) we felt that tagging the protein at the COOH-terminus would have no negative impact on its activity. The cDNA fragment encoding the HA-epitope- and histidine-tagged murine Timp-2 protein was subcloned into the doxycycline-responsive uni-directional expression plasmid pUHD 10-3 and the bi-directional expression plasmid pBI-3 which in addition to the tagged Timp-2 protein also encodes *β*-galactosidase with a nuclear localization signal (Fig. 1a). Stably transfected HeLa cells synthesized the tagged Timp-2 protein in an inducible fashion (Fig. 1b) and secreted it into the medium from which it could be easily purified over a nickel column (Fig. 1c). When the purified

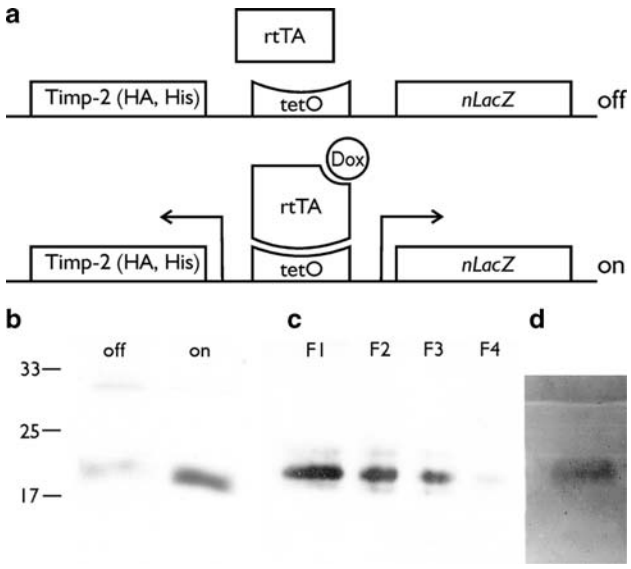

Fig. 1 Inducible production of a tagged Timp-2 protein. **a** Strategy. In the absence of doxycycline, the reverse tetracycline-dependent transactivator (rtTA) will not bind to tet-operator sequences (tetO) in the promotor region. Upon the addition of doxycycline, rtTA will bind and thereby activate the transcription of the Timp-2 cDNA and of the *nLacZ* gene. **b** Total cell lysates of stably transfected HeLa cells in the non-induced (off) and in the induced (on) state were analyzed by Western blot with the anti-HA-epitope antibody 12CA5. The epitope-tagged murine Timp-2 protein can be seen at the predicted size. **c** Stably transfected HeLa cells were induced, the cell culture supernatant was collected over 7 days and purified over a nickel column. After elution with imidazole, the first three fractions contain most of the epitope-tagged Timp-2 protein. **d** A reverse zymography assay demonstrates that the purified, epitope-tagged Timp-2 protein still inhibits matrix metalloproteinases

Timp-2 was subjected to a reverse zymography assay, it was still active (Fig. 1d) and we therefore went on to generate transgenic mice producing the tagged Timp-2 protein.

Transgenic mice

Out of 350 injected oocytes, 90 viable offspring were obtained. Genotyping led to the identification of 13 mice which contained the transgene and were subsequently mated to $rtTA^{LAP}$-1 mice. In the latter strain the S2 version of the reverse tetracycline-dependent transactivator is driven by the LAP (liver activator protein) promoter (Hasan et al. 2001; Schönig et al. 2002). After the addition of the tetracycline-analogue doxycycline, double-transgenic mice will show blue nuclei in proximal tubules upon histochemical staining for *β*-galactosidase with X-gal. Indeed, kidney sections from two out of the 13 lines contained very strong *β*-galactosidase activity in proximal tubules, and therefore one of them was subsequently crossed to $CD1^{pcy/pcy}$ mice. The $CD1^{pcy/pcy}$ line represents a recessive model of cystic kidney disease (Takahashi et al. 1986, 1991) and results from a spontaneous mutation in the *Nphp3* gene (Olbrich

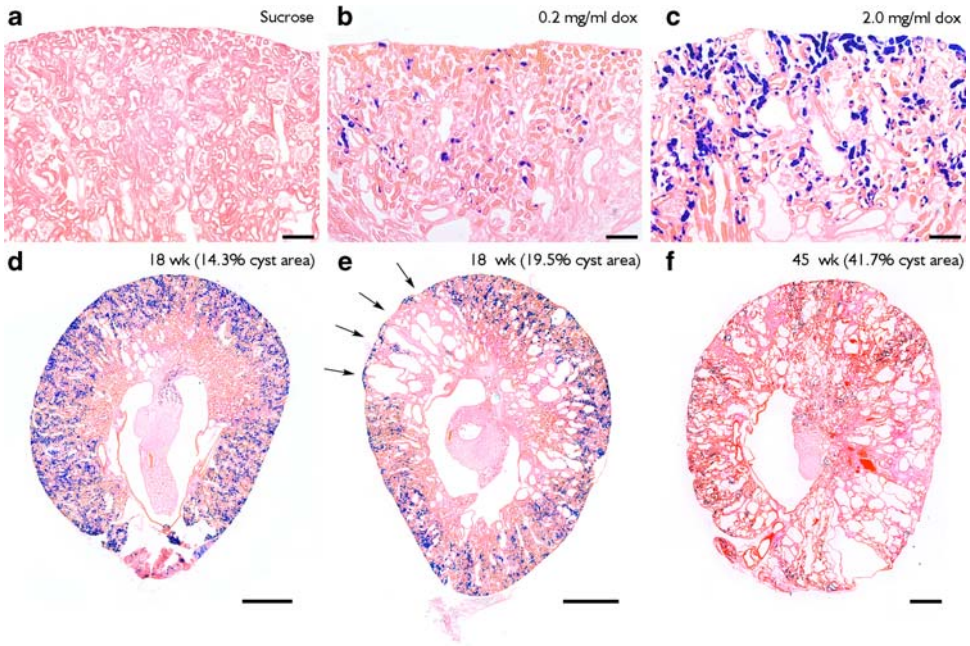

Fig. 2 Induction of β-galactosidase and Timp-2 in double-transgenic CD1$^{pcy/pcy}$ mice. **a–c** Double-transgenic CD1$^{pcy/pcy}$ mice were administered 5% sucrose (**a**), 5% sucrose together with 0.2 mg/ml of doxycycline (**b**) and 5% sucrose together with 2 mg/ml of doxycycline for 2 weeks. Histochemical staining for β-galactosidase and subsequent counterstaining with eosin reveals the dose-dependent induction of β-galactosidase. **d–f** The indicated animals received 5% sucrose together with 2 mg/ml of doxycycline for 2 weeks. It can be easily seen that β-galactosidase activity diminishes with increasing degree of cyst formation. The arrows in (**e**) indicate an area with a focal loss of β-galactosidase activity. *Bars*, 0.1 mm (**a–c**) and 1 mm (**d–f**)

et al. 2003). Cysts in CD1$^{pcy/pcy}$ mice develop preferentially in the cortex and the outer stripe, and the site of cyst formation therefore overlaps with the site of β-galactosidase activity (Fig. 2).

Double-transgenic CD1$^{pcy/pcy}$ mice (for sake of simplicity, henceforth this term indicates the presence of the expression cassettes for the reverse transactivator on the one side and for epitope-tagged Timp-2 and β-galactosidase on the other side) were administered doxycycline at concentrations of 0.2 and 2 mg/ml in the drinking water in order to find out what doxycycline concentration was necessary to induce β-galactosidase. Although blue nuclei were detected at 0.2 mg/ml, mice receiving the higher dose of doxycycline showed much more widespread β-galactosidase activity in the cortex (Fig. 2a–c) which confirmed our previous observations (Gallagher et al. 2003). We also noticed that the degree of β-galactosidase activity depended on how far cyst formation had progressed. The more cysts had developed, the less β-galactosidase activity was observed (Fig. 2d–f). Our attempts to visualize the Timp-2 protein by immunofluorescence and by Western blot of kidney extracts with various anti-HA epitope antibodies failed. On the other hand we were able to easily detect the Timp-2 and LacZ mRNAs by real-time PCR which yielded relative expression levels of 339 and 335 for the Timp-2 and LacZ mRNAs, respectively (mean values from two double-transgenic mice after 2 weeks of induction). Non-transgenic CD1$^{pcy/pcy}$ mice had values of 0.15 and 0.29 for Timp-2 and LacZ, respectively, which was close to the negative control in which no reverse transcriptase was included (0.02 and 0.01, respectively). We therefore conclude that the exogenous Timp-2 mRNA was produced but that the level of the exogenous protein was below the detection limit.

Cyst-lining epithelial cells typically did not produce β-galactosidase, but since Timp-2 is a secreted protein and cells positive for β-galactosidase were located in immediate vicinity to cysts we felt encouraged to investigate whether Timp-2 was able to slow down cyst formation. Starting at the age of 8 weeks, doxycycline was administered for 14 weeks in the drinking water at a concentration of 2 mg/ml to female CD1$^{pcy/pcy}$ mice (sucrose was included at a concentration of 5% to make the doxycycline more palatable). Mice were then killed by perfusion–fixation and the heart and both kidneys were removed and weighed. Contrary to what we expected, the absolute and relative kidney weights in the double-transgenic CD1$^{pcy/pcy}$ mice increased under administration of doxycycline compared to sucrose alone, whereas the heart weights were not changed significantly (Table 1). This indicated that the induction of Timp-2 accelerated cyst growth. Alternatively, doxycycline alone which was described to inhibit matrix metalloproteinases (Hanemaaijer et al. 2001; Smith and Hasty 2001) because

of its zinc-chelating properties may have had an effect on cyst formation. Therefore, CD1$^{pcy/pcy}$ mice containing only the rtTA and the Timp2/*nLacZ* cassettes, respectively, were also examined for an effect of doxycycline. Indeed, even in single-transgenic mice kidney weights increased drastically upon the administration of doxycycline (Table 1), thus arguing that the most important factor for the increased kidney weight was doxycycline and not Timp-2. This interpretation is supported by the fact that we did not measure a significant difference in the relative kidney weights between the double-transgenic mice and the single-transgenic mice, although there was a tendency toward higher relative kidney weights in the double-transgenic mice (Table 1). Morphometric analysis of the kidney sections demonstrated a higher cystic index in the double-transgenic and in the single-transgenic CD1$^{pcy/pcy}$ mice when doxycycline was administered. This effect was due to both an increase in the number of cysts and the average cyst size (Table 1). Besides its consequences on cyst growth, we noticed another negative consequence of doxycycline which may or may not be due to the increased rate of cyst formation. Staining of the kidney sections with Sirius red showed an increased deposition of connective tissue (Table 1).

We wanted to know whether the effect of doxycycline on kidney growth could also be observed in other mouse lines. Autosomal-recessive polycystic kidney disease is caused by mutations in the *PKHD1* gene which codes for a protein variably called fibrocystin and polyductin. *Pkhd1* knock-out mice lacking exon 4 of the murine orthologue develop hepatic cysts but no renal cysts (Gallagher et al. 2008). We tested whether doxycycline would be able to initiate cyst formation in the *Pkhd1* knock-out mice and administered doxycycline at a concentration of 2 mg/ml for 8 weeks starting at 1 month of age. Neither in the control group nor in the doxycycline-treated group of mice polycystic kidneys developed (Table 2). In another set of experiments, CD1$^{pcy/pcy}$ mice were backcrossed onto regular CD1 mice to generate heterozygous CD1$^{+/pcy}$ mice which do not develop cystic kidney disease. Again starting at 8 weeks of age and lasting for 14 weeks, doxycycline was administered to female mice in the drinking water at a concentration of 2 mg/ml. In those mice a slightly increased relative kidney weight was observed which can be explained by the decreased body weight upon doxycycline administration (Table 3).

Table 2 Doxycycline does not affect cyst growth in *Pkhd1* knock-out mice

	No dox	2.0 mg/ml dox
Body weight (g)	27.6 ± 4.9 (n = 3)	22.9 ± 2.7 (n = 5)
Kidney weight (g)	0.48 ± 0.14 (n = 3)	0.41 ± 0.05 (n = 5)
Kidney weight/ body weight (100×)	1.73 ± 0.21 (n = 3)	1.79 ± 0.15 (n = 5)
Relative cystic area (%)	3.77 ± 2.46 (n = 4)	3.77 ± 0.62 (n = 5)

Pkhd1 knock-out mice received 5% sucrose (no dox) or 5% sucrose together with 2 mg/ml of doxycycline (2.0 mg/ml dox). Values represent the mean ± standard deviation. No statistically significant differences were observed

Possible effects underlying increased cyst formation upon administration of doxycycline

In order to learn more about the mechanism through which doxycycline led to increased cyst formation, CD1$^{pcy/pcy}$

Table 1 The administration of doxycycline leads to increased cyst formation and fibrosis in CD1$^{pcy/pcy}$ mice

	rtTA/Timp-2		rtTA		Timp-2	
	No dox	2.0 mg/ml dox	No dox	2.0 mg/ml dox	No dox	2.0 mg/ml dox
Body weight (g)	23.2 ± 1.8	19.6 ± 1.7$^{\#}$	22.9 ± 1.6	20.7 ± 1.7*	21.4 ± 0.7	19.9 ± 1.7*
Kidney weight (g)	0.30 ± 0.08	0.52 ± 0.09$^{\#}$	0.31 ± 0.09	0.49 ± 0.15*	0.26 ± 0.06	0.38 ± 0.14*
Kidney weight/ body weight (100×)	2.44 ± 0.56	5.10 ± 0.77$^{\#}$	2.55 ± 0.77	4.40 ± 1.42$^{\#}$	2.29 ± 0.40	3.90 ± 1.56$^{\#}$
Heart weight (g)	0.13 ± 0.02	0.10 ± 0.01*	0.14 ± 0.03	0.11 ± 0.02*	0.14 ± 0.03	0.11 ± 0.01*
Heart weight/ body weight, (1,000×)	5.65 ± 0.65	5.32 ± 0.67	6.09 ± 0.93	5.31 ± 0.59	6.54 ± 1.09	5.69 ± 0.51
Relative cystic area (%)	14.8 ± 7.5	30.9 ± 7.1$^{\#}$	13.0 ± 9.2	27.8 ± 10.3$^{\#}$	14.8 ± 7.5	24.0 ± 11.7$^{\#}$
Cyst number	96 ± 49	171 ± 36$^{\#}$	97 ± 47	149 ± 56*	75 ± 38	133 ± 54$^{\#}$
Cyst size (μm^2)	28,743 ± 6,747	39,416 ± 8,336$^{\#}$	29,857 ± 7,458	40,534 ± 13,136$^{\#}$	31,013 ± 8,626	36,671 ± 12,868
Relative fibrotic area (%)	4.23 ± 3.70	10.38 ± 3.43$^{\#}$	3.56 ± 2.56	9.99 ± 4.79$^{\#}$	3.64 ± 2.66	8.38 ± 5.01$^{\#}$

CD1$^{pcy/pcy}$ mice containing both the rtTA and Timp-2/*nLacZ* cassettes (rtTA/Timp-2), only the rtTA (rtTA) or only the Timp-2/*nLacZ* cassettes (Timp-2) were included in the experiment. The animals received 5% sucrose (no dox) or 5% sucrose together with 2 mg/ml of doxycycline (2.0 mg/ml dox). Values represent the mean ± standard deviation from seven animals each. $^{*}P \leq 0.05$; $^{\#}P \leq 0.01$

Table 3 Doxycycline only affects the relative but not the absolute kidney weights of CD1$^{+/pcy}$ mice

	No dox	2.0 mg/ml dox
Body weight (g)	31.9 ± 3.0	29.6 ± 3.2
Kidney weight (g)	0.21 ± 0.03	0.22 ± 0.03
Kidney weight/ body weight (100×)	1.32 ± 0.12	1.47 ± 0.15*
Heart weight (g)	0.17 ± 0.02	0.15 ± 0.02
Heart weight/ body weight (1,000×)	5.35 ± 1.02	5.21 ± 0.49

CD1$^{+/pcy}$ mice received 5% sucrose (no dox) or 5% sucrose together with 2 mg/ml of doxycycline (2.0 mg/ml dox). Values represent the mean ± standard deviation from 10 animals each. *$P \leq 0.05$

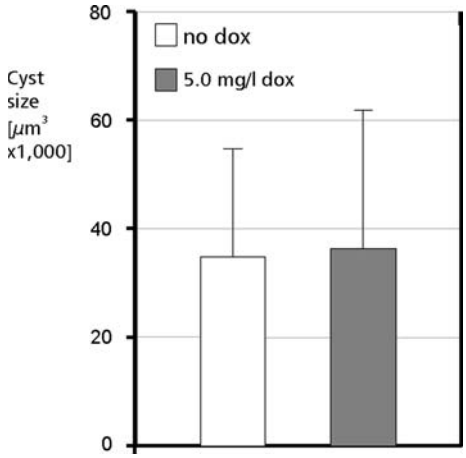

Fig. 3 Cyst formation in collagen gels. A total of 300,000 cells were cultured in a collagen gel poured at a concentration of 2.5 mg/ml of collagen to allow the formation of cysts. After 7 days, no difference can be seen between culturing the collagen gels without and with doxycycline

mice were given doxycycline in the drinking water at a concentration of 2 mg/ml for 2 weeks. HPLC measurements of the doxycycline concentration in kidney extracts and serum yielded values of 5.2 ± 3.5 mg/kg in the kidney and of 1.0 ± 0.5 mg/l in the serum (mean ± SD, $n = 7$ animals). These values are consistent with the doxycycline concentration of 1 mg/l which is routinely used to activate the reverse tetracycline-dependent transactivator in cell culture (Urlinger et al. 2000). We next established primary cultures from kidneys of CD1$^{pcy/pcy}$ mice and grew them in collagen gels using different parameters: cell densities ranged from 5×10^4 to 3×10^5 cells/ml, collagen concentration varied between 1 and 2.5 mg/ml, and cells were cultured for 7–14 days. Both tubular and cystic structures were observed under these conditions (cystic structures were more common when primary cultures were established from older animals) but the number and size did not change when doxycycline was added. With a collagen concentration of 2.5 mg/ml and a cell density of 3×10^5 cells/ml, the average cyst volume with and without 5 mg/l of doxycycline did not differ (Fig. 3).

Primary cilia, thread-like singular extensions of the luminal plasma membrane, are felt to represent an essential link in the pathogenesis of cystic kidney diseases. Both mechano- (Nauli et al. 2003; Praetorius and Spring 2001) and chemosensory (Barr et al. 2001; Barr and Sternberg 1999; Haycraft et al. 2001) roles have been proposed for primary cilia but at the current state of knowledge it is not clear how primary cilia determine the width of the renal tubules (Witzgall 2005). We reasoned that the administration of doxycycline rather resulted in a change of the chemical environment of tubular epithelial cells. Since tubular fluid is not available in sufficient quantities we instead resorted to collecting urine as a substitute. To this end, mice were kept in metabolic cages for 22 h after the 10-day long administration of doxycycline plus sucrose and of sucrose only. Indeed, the urine of sucrose-treated animals elicited a much stronger rise of $[Ca^{2+}]_i$ in LLC-PK$_1$ cells than that of doxycycline-treated animals (Fig. 4a). This effect could have been due to the induction of an inhibitory substance or to the suppression of an activating substance by doxycycline. When we incubated the urine of doxycycline-treated CD1$^{pcy/pcy}$ mice with proteinase K or incubated it for 15 min at 95°C prior to adding it to LLC-PK$_1$ cells, we still observed a drop in intracellular calcium levels (Fig. 4b–d). This prompted us to examine whether the addition of doxycycline to the urine of sucrose-treated CD1$^{pcy/pcy}$ mice inhibited the calcium response of LLC-PK$_1$ cells but it did not (Fig. 4e, f). Proteinase K also had no effect (Fig. 4g) but incubation at 95°C abrogated the rise in $[Ca^{2+}]_i$ (Fig. 4h). Finally, when we mixed urine samples of doxycycline- and sucrose-treated animals we again observed a drop in the intracellular calcium concentration (Fig. 5). This suggests that the urine of CD1$^{pcy/pcy}$ mice contains a heat-labile, non-proteinaceous stimulatory substance whose effect, however, is blocked through the induction of a heat-stable, nonproteinaceous substance by doxycycline.

In order to look for other changes in the urine which we might miss in our assay using LLC-PK$_1$ cells we also looked into the urinary excretion of proteins. Urine was collected from CD1$^{pcy/pcy}$ mice which had received 2 mg/ml of doxycycline together with 5% sucrose or only 5% sucrose for 17 days. Upon denaturing polyacrylamide gel electrophoresis we observed a strong downregulation of a band with ~18 kDa in size and the upregulation of a band with ~62 kDa in size (Fig. 6). The respective bands were cut out, digested with trypsin, and subjected to mass spectrometry. This allowed us to identify the high molecular weight band as albumin and the lower molecular weight band as major urinary proteins (MUPs).

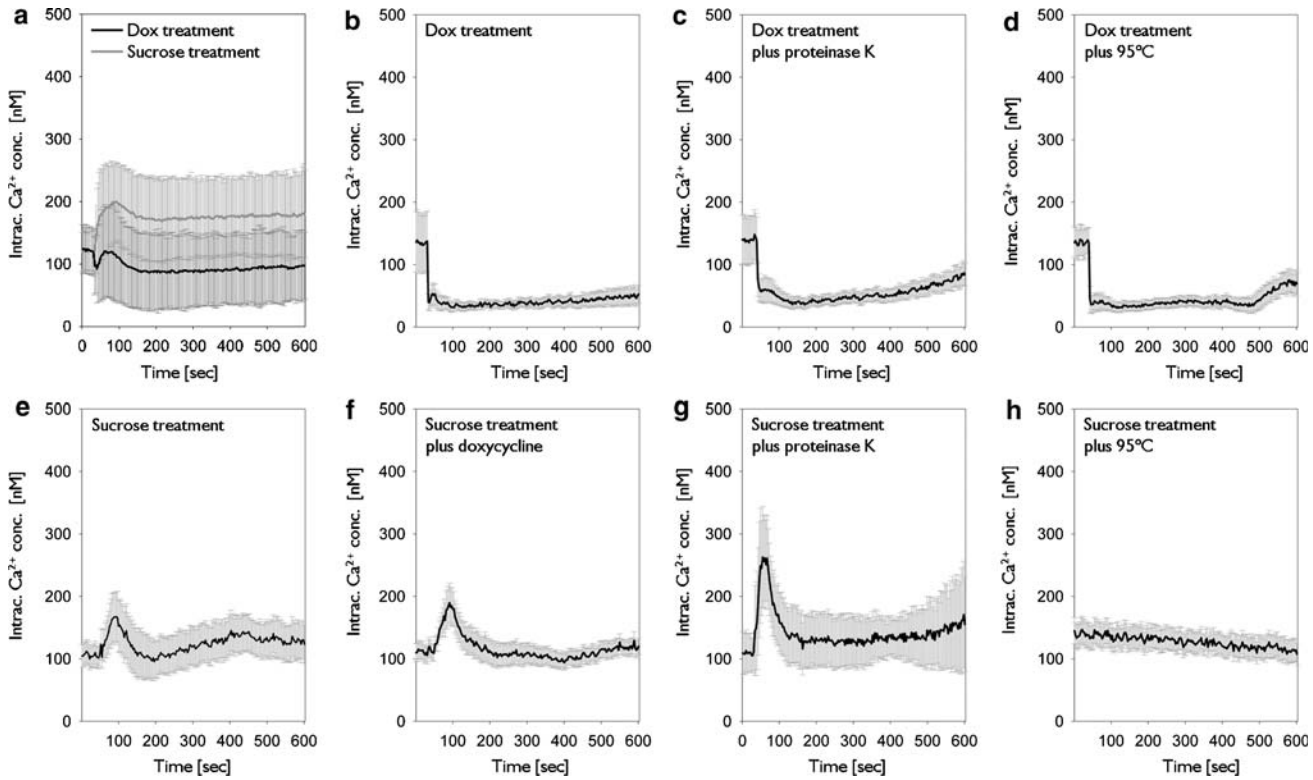

Fig. 4 Calcium response of LLC-PK$_1$ cells. **a** Urine was collected for 10 days from four CD1$^{pcy/pcy}$ mice exposed to 2 mg/ml of doxycycline and 5% sucrose (Dox treatment) and from five CD1$^{pcy/pcy}$ mice exposed to 5% sucrose only (Sucrose treatment). When LLC-PK$_1$ cells were exposed to urine of these mice (diluted to 5% in imaging buffer) the urine of doxycycline-treated mice caused an impaired calcium response. **b**–**d** This impaired calcium response (**b**) can even be observed after incubating the urine with proteinase K (**c**) and after heat treatment (**d**). **e**–**h** Neither the addition of doxycycline to a concentration of 5 mg/l (**f**) nor the incubation with proteinase K (**g**) prevented the rise in $[Ca^{2+}]_i$ caused by urine from sucrose-fed mice, but heat treatment completely abrogated it (**h**)

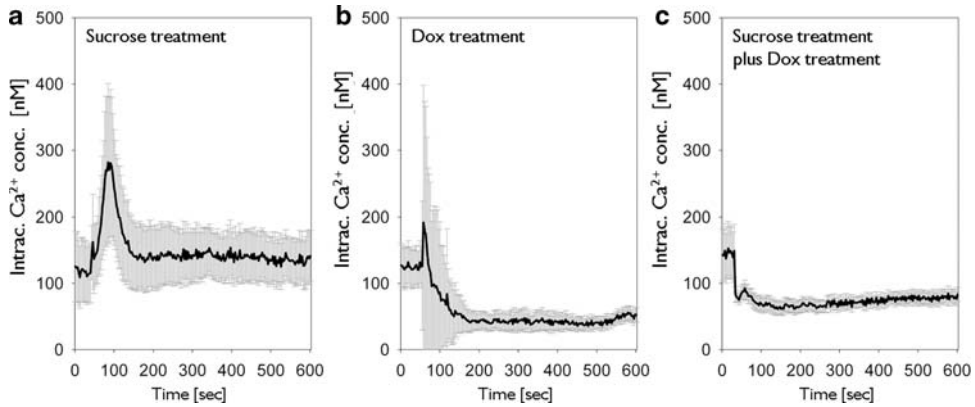

Fig. 5 The urine of doxycycline-treated mice overrides the positive effect caused by the urine of sucrose-treated mice. Urine from sucrose-treated mice diluted to a final concentration of 2.5% (v/v) in the imaging buffer caused a rise in $[Ca^{2+}]_i$ (**a**) but the urine of doxycycline-treated animals did not (**b**). The positive effect of the urine from sucrose-treated animals was overridden when urine from doxycycline-treated animals was added to an equal concentration (**c**)

Discussion

Tetracycline derivatives such as doxycycline have been reported to inhibit MMPs which is why we started our study by investigating the efficiency of *nLacZ* induction using doxycycline at 0.2 and 2 mg/ml. We wanted to use as low a concentration of doxycycline as possible in order to avoid any unwanted side effects. Since the lower concentration showed only an inefficient induction of *nLacZ* we focussed our investigation on mice treated with 2 mg/ml of doxycycline. The levels obtained in the kidney (~5 mg doxycycline/kg kidney weight) are in a concentration range

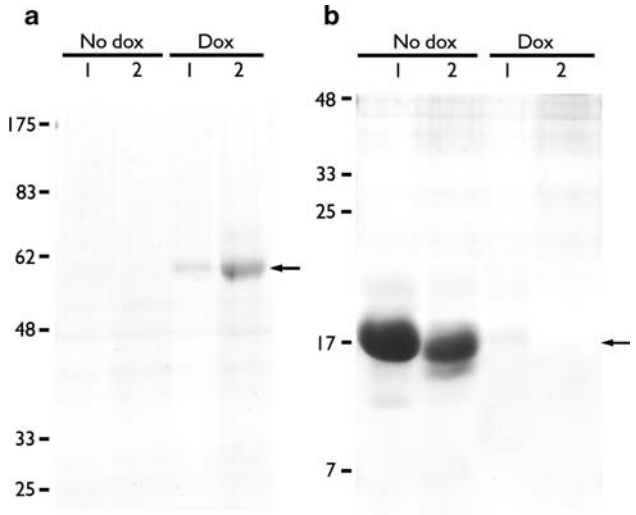

Fig. 6 The administration of doxycycline leads to the increased urinary excretion of albumin and the decreased urinary excretion of major urinary proteins (MUPs). Urine aliquots from sucrose (No dox)- and doxycycline (Dox)-treated male mice containing 10 μg of total protein were run on 10% (**a**) and 16% (**b**) polyacrylamide gels under denaturing and reducing conditions. The indicated bands (*arrows*) were cut out and subjected to mass spectrometry which revealed that they represented albumin (**a**) and major urinary proteins (MUPs) (**b**). Molecular masses in kDa are given on the left of each gel

which is able to inhibit the synthesis and enzymatic activity of MMPs (Hanemaaijer et al. 2001; Smith and Hasty 2001) so we were aware that we might observe a Timp-2-independent effect of doxycycline. What we had not expected, however, was that doxycycline accelerated cyst growth—if anything, we would have predicted an additive, inhibitory effect together with Timp-2. The fact that we were not able to see an additional effect of Timp-2 may be attributed to the strong influence of doxycycline and/or the low level of Timp-2 in our transgenic mice. As far as it is possible to compare two different mRNA levels by quantitative PCR we saw equal levels of Timp-2 mRNA and LacZ mRNA, but obviously the histochemical reaction for β-galactosidase is much more sensitive that the immunofluorescence for Timp-2 because we could only detect the former and not the latter protein.

How doxycycline enhances cyst formation has to remain a matter of speculation right now. When we subjected primary kidney cells of CD1$^{pcy/pcy}$ mice to a cyst-forming assay in collagen gels we detected neither a positive nor a negative effect of 5 mg/l of doxycycline on cyst formation. The absence of an effect may be explained by the comparably short culture period (only up to 14 days) which is technically possible in collagen gels as opposed to the long treatment of the mice (14 weeks). Another obvious difference between the in vitro and the in vivo situation is the absence of fluid flow in the collagen gels. Arguments have been presented that primary cilia serve as mechanosensors on renal tubular epithelial cells (Nauli et al. 2003; Praetorius and Spring 2001) but both for theoretical reasons (Witzgall 2005) and from experimental evidence (Davenport et al. 2007; Köttgen et al. 2008; Piontek et al. 2007) doubts have been presented against such a model. What we did observe was that the urine of placebo-treated CD1$^{pcy/pcy}$ mice contains a heat-labile, probably non-proteinaceous substance that induces a rise in the intracellular calcium concentration of LLC-PK$_1$ cells. Several publications have provided evidence that a reduced $[Ca^{2+}]_i$ contributes to cyst formation (Nagao et al. 2008; Nauli et al. 2003; Yamaguchi et al. 2006) which is consistent with the effect observed by us.

Alternatively the tubular geometry could also be determined by the concentration of a so far hypothetical substance in the tubular fluid (Witzgall 2005). What this substance may be is not clear but we want to point out studies undertaken by the Grantham group which has isolated a lipophilic forskolin-like molecule in human renal cyst fluid (Putnam et al. 2007). Forskolin and the forskolin-like molecule cause an increase in the intracellular cAMP concentration and therefore probably are different from the substance leading to a positive calcium response. However, we have observed in our study that the urine of doxycycline-treated CD1$^{pcy/pcy}$ mice prevented the rise in $[Ca^{2+}]_i$ and rather led to a drop in $[Ca^{2+}]_i$. We would argue that doxycycline induced the synthesis of a substance which overrode the positive effect of a molecule (or molecules) in the urine of placebo-treated mice. Regrettably we do not know what the nature of such a substance may be. In this context we want to point out the intriguing observation that doxycycline administration led to a massive downregulation of MUPs in the urine. MUPs are excreted both by male and female mice (female/male output ~30%) and can bind a wide variety of low molecular mass substances (Beynon and Hurst 2004). Whether the decreased urinary excretion of MUPs after the administration of doxycycline is connected to the accelerated cyst formation or is just an epiphenomenon will have to be the subject of further investigations.

We admit that although primary cilia are involved in chemosensation (Barr et al. 2001; Barr and Sternberg 1999; Haycraft et al. 2001) our results describing the effects of urine on the intracellular calcium concentration in LLC-PK$_1$ cells may be unrelated to the underlying pathomechanism. Another tempting speculation how doxycycline accelerates cyst growth is based on observations that polycystin-1 and fibrocystin/polyductin, the proteins mutated in patients suffering from type 1 autosomal-dominant and autosomal-recessive polycystic kidney disease, respectively, undergo proteolytic processing (Hiesberger et al. 2006; Kaimori et al. 2007; Qian et al. 2002). At least for polycystin-1 proteolytic processing is necessary for the protein to fulfil its function because genetically modified mice

which cannot cleave off the extracellular domain of polycystin-1 develop polycystic kidney disease (Yu et al. 2007). The proteases responsible for the processing of polycystin-1 and fibrocystin/polyductin are unknown but in the case of fibrocystin/polyductin it is likely that a metalloproteinase is involved (Kaimori et al. 2007). Furthermore we want to point out that the processing of fibrocystin/polyductin depends on intracellular calcium (Hiesberger et al. 2006). At present the function of nephrocystin-3, the protein mutated in CD1$^{pcy/pcy}$ mice, is unclear but even if it is not connected with polycystin-1 and fibrocystin/polyductin it may well be that doxycycline prevents the cleavage of the two latter proteins and thus exacerbates cystic kidney disease in CD1$^{pcy/pcy}$ mice. Our result that doxycycline did not initiate cyst formation in *Pkhd1*$^{del4/del4}$ knock-out mice does not rule out such an interpretation because fibrocystin/polyductin will be inactive already in those mice and doxycycline would have no additional effect if it acted through fibrocystin/polyductin. The finding that doxycycline neither induced cyst formation in the *Pkhd1*$^{del4/del4}$ knock-out mice (which only develop polycystic liver but not polycystic kidney disease) nor in the CD1$^{+/pcy}$ mice suggests that it acts as an aggravating but not as an initiating factor.

The other negative effect we observed after application of doxycycline was increased renal fibrosis. Fibrosis is not only a consequence of renal damage but also leads to further kidney injury. A correlation between decreased Mmp-1, Mmp-2, and Mmp-9 activity and renal fibrosis has been reported in two independent studies (Maric et al. 2004; Uchio et al. 2000) and it is therefore conceivable that doxycycline impaired the turnover of the extracellular matrix and led to tubulointerstitial fibrosis. Taken together, the results of our current study for the first time demonstrate the adverse effects of doxycycline on the course of polycystic kidney disease. It remains to be seen whether doxycycline also enhances cyst growth in other animal models in addition to CD1$^{pcy/pcy}$ mice but our results caution against the long-term administration of doxycycline in patients suffering from certain forms of polycystic kidney disease such as type 3 nephronophthisis.

Acknowledgments The murine Timp-2 cDNA was kindly provided by Dylan Edwards. Ulrike Haas and Nicole Maltry engineered the expression plasmids for the epitope-tagged Timp-2 protein and generated the stably transfected cell lines. Rainer Deutzmann performed the mass spectrometry analysis. We also want to thank Frank Zimmermann and Sascha Dlugosz for performing the microinjections to establish the transgenic mice, and we are grateful to Ton Maurer for photographic work and arrangement of the figures. Our study received generous financial support from the Else Kröner-Fresenius-Stiftung (P15/05//A20/05//F00) and from the European Union (QLRT-2000-01104).

Conflict of interest The authors declare no conflict of interest.

References

Abramoff MD, Magelhaes PJ, Ram SJ (2004) Image processing with ImageJ. Biophotonics Int 11:36–42

Ausubel FA, Brent R, Kingston RE, Moore DD, Seidman JG, Smith JA, Struhl K (1996) Current protocols in molecular biology. Wiley & Sons, New York

Baron U, Freundlieb S, Gossen M, Bujard H (1995) Co-regulation of two gene activities by tetracycline via a bidirectional promoter. Nucleic Acids Res 23:3605–3606

Barr MM, Sternberg PW (1999) A polycystic kidney-disease gene homologue required for male mating behaviour in *C. elegans*. Nature 401:386–389

Barr MM, DeModena J, Braun D, Nguyen CQ, Hall DH, Sternberg PW (2001) The *Caenorhabditis elegans* autosomal dominant polycystic kidney disease gene homologs *lov-1* and *pkd-2* act in the same pathway. Curr Biol 11:1341–1346

Bello-Reuss E, Holubec K, Rajaraman S (2001) Angiogenesis in autosomal-dominant polycystic kidney disease. Kidney Int 60:37–45

Beynon RJ, Hurst JL (2004) Urinary proteins and the modulation of chemical scents in mice and rats. Peptides 25:1553–1563

Catania JM, Chen G, Parrish AR (2007) Role of matrix metalloproteinases in renal pathophysiologies. Am J Physiol Renal Physiol 292:F905–F911

Cinquina AL, Longo F, Anastasi G, Giannetti L, Cozzani R (2003) Validation of a high-performance liquid chromatography method for the determination of oxytetracycline, tetracycline, chlortetracycline and doxycycline in bovine milk and muscle. J Chromatogr A 987:227–233

Davenport JR, Watts AJ, Roper VC, Croyle MJ, van Groen T, Wyss JM, Nagy TR, Kesterson RA, Yoder BK (2007) Disruption of intraflagellar transport in adult mice leads to obesity and slow-onset cystic kidney disease. Curr Biol 17:1586–1594

Dell KM, Nemo R, Sweeney WE Jr, Levin JI, Frost P, Avner ED (2001) A novel inhibitor of tumor necrosis factor-α converting enzyme ameliorates polycystic kidney disease. Kidney Int 60:1240–1248

Dong Y, Skoultchi AI, Pollard JW (1993) Efficient DNA transfection of quiescent mammalian cells using poly-L-ornithine. Nucleic Acids Res 21:771–772

Gallagher AR, Schönig K, Brown N, Bujard H, Witzgall R (2003) Use of the tetracycline system for inducible protein synthesis in the kidney. J Am Soc Nephrol 14:2042–2051

Gallagher A-R, Esquivel EL, Briere TS, Tian X, Mitobe M, Menezes LF, Markowitz GS, Jain D, Onuchic LF, Somlo S (2008) Biliary and pancreatic dysgenesis in mice harboring a mutation in *Pkhd1*. Am J Pathol 172:417–429

Gardner KD Jr, Burnside JS, Elzinga LW, Locksley RM (1991) Cytokines in fluids from polycystic kidneys. Kidney Int 39:718–724

Hanemaaijer R, van Lent N, Sorsa T, Salo T, Konttinen YT, Lindeman J (2001) Inhibition of matrix metalloproteinases (MMPs) by tetracyclines. In: Nelson M, Hillen W, Greenwald RA (eds) Tetracyclines in biology chemistry and medicine. Birkhäuser Verlag, Switzerland, pp 267–281

Hasan MT, Schönig K, Berger S, Graewe W, Bujard H (2001) Long-term, noninvasive imaging of regulated gene expression in living mice. Genesis 29:116–122

Haycraft CJ, Swoboda P, Taulman PD, Thomas JH, Yoder BK (2001) The *C. elegans* homolog of the murine cystic kidney disease gene *Tg737* functions in a ciliogenic pathway and is disrupted in *osm-5* mutant worms. Development 128:1493–1505

Hiesberger T, Gourley E, Erickson A, Koulen P, Ward CJ, Masyuk TV, Larusso NF, Harris PC, Igarashi P (2006) Proteolytic cleavage and nuclear translocation of fibrocystin is regulated

by intracellular Ca^{2+} and activation of protein kinase C. J Biol Chem 281:34357–34364

Kaimori J-Y, Nagasawa Y, Menezes Y, Garcia-Gonzalez MA, Deng J, Imai E, Onuchic LF, Guay-Woodford LM, Germino GG (2007) Polyductin undergoes notch-like processing and regulated release from primary cilia. Hum Mol Genet 16:942–956

Kees F, Dehner R, Dittrich W, Raasch W, Grobecker H (1990) The bioavailability of doxycycline. Arzneimittelforschung 40:1039–1043

Köttgen M, Buchholz B, Garcia-Gonzalez MA, Kotsis F, Fu X, Doerken M, Boehlke C, Steffl D, Tauber R, Wegierski T, Nitschke R, Suzuki M, Kramer-Zucker A, Germino GG, Watnick T, Prenen J, Nilius B, Kuehn EW, Walz G (2008) TRPP2 and TRPV4 form a polymodal sensory channel complex. J Cell Biol 182:437–447

Leco KJ, Hayden LJ, Sharma RR, Rocheleau H, Greenberg AH, Edwards DR (1992) Differential regulation of *TIMP-1* and *TIMP-2* mRNA expression in normal and Ha-*ras*-transformed murine fibroblasts. Gene 117:209–217

Maric C, Sandberg K, Hinojosa-Laborde C (2004) Glomerulosclerosis and tubulointerstitial fibrosis are attenuated with 17b-estradiol in the aging Dahl salt sensitive rat. J Am Soc Nephrol 15:1546–1556

Murphy G, Houbrechts A, Cockett MI, Williamson RA, O'Shea M, Docherty AJP (1991) The N-terminal domain of tissue inhibitor of metalloproteinases retains metalloproteinase inhibitory activity. Biochemistry 30:8097–8102

Nagao S, Nishii K, Yoshihara D, Kurahashi H, Nagaoka K, Yamashita T, Takahashi H, Yamaguchi T, Calvet JP, Wallace DP (2008) Calcium channel inhibition accelerates polycystic kidney disease progression in the Cy/+ rat. Kidney Int 73:269–277

Nauli SM, Alenghat FJ, Luo Y, Williams E, Vassilev P, Li X, Elia AEH, Lu W, Brown EM, Quinn SJ, Ingber DE, Zhou J (2003) Polycystins 1 and 2 mediate mechanosensation in the primary cilium of kidney cells. Nat Genet 33:129–137

Norman JT, Gatti L, Wilson PD, Lewis M (1995) Matrix metalloproteinases and tissue inhibitor of matrix metalloproteinases expression by tubular epithelia and interstitial fibroblasts in the normal kidney and in fibrosis. Exp Nephrol 3:88–89

Obermüller N, Morente N, Kränzlin B, Gretz N, Witzgall R (2001) A possible role for metalloproteinases in renal cyst development. Am J Physiol Renal Physiol 280:F540–F550

Olbrich H, Fliegauf M, Hoefele J, Kispert A, Otto E, Volz A, Wolf MT, Sasmaz G, Trauer U, Reinhardt R, Sudbrak R, Antignac C, Gretz N, Walz G, Schermer B, Benzing T, Hildebrandt F, Omran H (2003) Mutations in a novel gene, *NPHP3*, cause adolescent nephronophthisis, tapeto-retinal degeneration and hepatic fibrosis. Nat Genet 34:455–459

Piedagnel R, Murphy G, Ronco PM, Lelongt B (1999) Matrix metalloproteinase 2 (MMP2) and MMP9 are produced by kidney collecting duct principal cells but are differentially regulated by SV40 large-T, arginine vasopressin, and epidermal growth factor. J Biol Chem 274:1614–1620

Piontek K, Menezes LF, Garcia-Gonzalez MA, Huso DL, Germino GG (2007) A critical developmental switch defines the kinetics of kidney cyst formation after loss of *Pkd1*. Nat Med 13:1490–1495

Praetorius HA, Spring KR (2001) Bending the MDCK cell primary cilium increases intracellular calcium. J Membr Biol 184:71–79

Putnam WC, Swenson SM, Reif GA, Wallace DP, Helmkamp GM Jr, Grantham JJ (2007) Identification of a forskolin-like molecule in human renal cysts. J Am Soc Nephrol 18:934–943

Qian F, Boletta A, Bhunia AK, Xu H, Liu L, Ahrabi AK, Watnick TJ, Zhou F, Germino GG (2002) Cleavage of polycystin-1 requires the receptor for egg jelly domain and is disrupted by human autosomal-dominant polycystic kidney disease 1-associated mutations. Proc Natl Acad Sci USA 99:16981–16986

Rankin CA, Suzuki K, Itoh Y, Ziemer DM, Grantham JJ, Calvet JJ, Nagase H (1996) Matrix metalloproteinases and TIMPs in cultured C57BL/6J-*cpk* kidney tubules. Kidney Int 50:835–844

Rankin CA, Itoh Y, Tian C, Ziemer DM, Calvet JP, Gattone VHII (1999) Matrix metalloproteinase-2 in a murine model of infantile-type polycystic kidney disease. J Am Soc Nephrol 10:210–217

Riera M, Burtey S, Fontés M (2006) Transcriptome analysis of a rat PKD model: importance of genes involved in extracellular matrix metabolism. Kidney Int 69:1558–1563

Ronco P, Chatziantoniou C (2008) Matrix metalloproteinases and matrix receptors in progression and reversal of kidney disease: therapeutic perspectives. Kidney Int 74:873–878

Sato H, Takino T, Okada Y, Cao J, Shinagawa A, Yamamoto E, Seiki M (1994) A matrix metalloproteinase expressed on the surface of invasive tumour cells. Nature 370:61–65

Schaefer L, Han X, Gretz N, Häfner C, Meier K, Matzkies F, Schaefer RM (1996) Tubular gelatinase A (MMP-2) and its tissue inhibitors in polycystic kidney disease in the Han:SPRD rat. Kidney Int 49:75–81

Schönig K, Schwenk F, Rajewsky K, Bujard H (2002) Stringent doxycycline dependent control of CRE recombinase in vivo. Nucleic Acids Res 30:e134

Smith GN Jr, Hasty KA (2001) Structure/function studies of doxycycline effects on matrix metalloproteinase activity and cartilage degeneration. In: Nelson M, Hillen W, Greenwald RA (eds) Tetracyclines in biology, chemistry and medicine. Birkhäuser Verlag, Switzerland, pp 283–293

Strongin AY, Collier I, Bannikov G, Marmer BL, Grant GA, Goldberg GI (1995) Mechanism of cell surface activation of 72-kDa type IV collagenase. Isolation of the activated form of the membrane metalloprotease. J Biol Chem 270:5331–5338

Surendran K, Simon T, Liapis H, McGuire JK (2004) Matrilysin (MMP-7) expression in renal tubular damage: Association with *Wnt4*. Kidney Int 65:2212–2222

Sweeney WE Jr, Chen Y, Nakanishi K, Frost P, Avner ED (2000) Treatment of polycystic kidney disease with a novel tyrosine kinase inhibitor. Kidney Int 57:33–40

Takahashi H, Ueyama Y, Hibino T, Kuwahara Y, Suzuki S, Hioki K, Tamaoki N (1986) A new mouse model of genetically transmitted polycystic kidney disease. J Urol 135:1280–1283

Takahashi H, Calvet JP, Dittemore-Hoover D, Yoshida K, Grantham JJ, Gattone VH (1991) A hereditary model of slowly progressive polycystic kidney disease in the mouse. J Am Soc Nephrol 1:980–989

Torres VE, Sweeney WE Jr, Wang X, Qian Q, Harris PC, Frost P, Avner ED (2003) EGF receptor tyrosine kinase inhibition attenuates the development of PKD in Han:SPRD rats. Kidney Int 64:1573–1579

Uchio K, Manabe N, Tamura K, Miyamoto M, Yamaguchi M, Ogura A, Yamamoto Y, Miyamoto H (2000) Decreased matrix metalloproteinase activity in the kidneys of hereditary nephrotic mice (ICGN strain). Nephron 86:145–151

Urlinger S, Baron U, Thellmann M, Hasan MT, Bujard H, Hillen W (2000) Exploring the sequence space for tetracycline-dependent transcriptional activators: novel mutations yield expanded range and sensitivity. Proc Natl Acad Sci USA 97:7963–7968

Visse R, Nagase H (2003) Matrix metalloproteinases and tissue inhibitors of metalloproteinases. Structure, function, and biochemistry. Circ Res 92:827–839

Wang Z, Juttermann R, Soloway PD (2000) TIMP-2 is required for efficient activation of proMMP-2 in vivo. J Biol Chem 275:26411–26415

Witzgall R (2005) New developments in the field of cystic kidney diseases. Curr Mol Med 5:455–465

Yamaguchi T, Hempson SJ, Reif GA, Hedge A-M, Wallace DP (2006) Calcium restores a normal proliferation phenotype in human polycystic kidney disease epithelial cells. J Am Soc Nephrol 17:178–187

Yu S, Hackmann K, Gao J, He X, Piontek K, García González MA, Menezes LF, Xu H, Germino GG, Zuo J, Qian F (2007) Essential role of cleavage of polycystin-1 at G protein-coupled receptor proteolytic site for kidney tubular structure. Proc Natl Acad Sci USA 104:18688–18693